

Citation for published version:

Xiong, F, Sun, J, Cole, M, Guo, W, Yan, C, Dong, Y, Wang, L, Du, Z, Guo, T & Yan, O 2022, 'GaN LEDs with in situ synthesized transparent graphene heat-spreading electrodes fabricated by PECVD and penetration etching', *Journal of Materials Chemistry C*, vol. 10, no. 17, pp. 6794-6804 . <https://doi.org/10.1039/d1tc05279a>

DOI:

[10.1039/d1tc05279a](https://doi.org/10.1039/d1tc05279a)

Publication date:

2022

Document Version

Peer reviewed version

[Link to publication](#)

University of Bath

Alternative formats

If you require this document in an alternative format, please contact:
openaccess@bath.ac.uk

General rights

Copyright and moral rights for the publications made accessible in the public portal are retained by the authors and/or other copyright owners and it is a condition of accessing publications that users recognise and abide by the legal requirements associated with these rights.

Take down policy

If you believe that this document breaches copyright please contact us providing details, and we will remove access to the work immediately and investigate your claim.

Graphene / GaN LEDs: In-situ synthesized Transparent Graphene Heat-Spreading Electrodes

Fangzhu Xiong¹, Jie Sun^{2,*}, Matthew T. Cole,³ Weiling Guo^{1,*}, Chunli Yan⁴, Yibo Dong¹, Le Wang¹, Zaifa Du¹, Tailiang Guo², Qun Yan²

1 Key Laboratory of Optoelectronics Technology, College of Microelectronics, Beijing University of Technology, Beijing 100124, China

2 Fujian Science & Technology Innovation Laboratory for Optoelectronic Information of China, and College of Physics and Information Engineering of Fuzhou University, Fuzhou 350100, China

3 Department of Electronic and Electrical Engineering, University of Bath, Bath BA120BN, United Kingdom

4 Department of Information and Automation, Library of Fuzhou University, Fuzhou 350108, China

* Corresponding authors: guoweiling@bjut.edu.cn (W.G.); jie.sun@fzu.edu.cn (J.S.)

Abstract:

Here a technique for the in-situ growth of patterned graphene directly onto GaN LED epiwafers is introduced. Pre-patterned sacrificial Co acts as both an etching mask for the GaN and a catalyst for graphene growth. The use of plasma enhanced chemical vapor deposition reduces the graphene growth temperature ($\Delta T = \dots$ °C) and improves the material quality, where highly crystalline graphene can be obtained in just 2 min at 600 °C. This method can directly pattern graphene without using additional lithographic steps and in doing so avoids unintentional deleterious doping and damage of the graphene. The approach simplifies fabrication and enhances device yield, process by eliminating the need for troublesome, manual, lengthy, and irreproducible graphene transfer procedures. By comparing GaN LEDs with and without graphene, we find that the graphene greatly improves the device optical, electrical and thermal performances, due to the high optical transparency (measured %) and high heat spreading capability of the graphene electrode. Unlike previous works using mechanically transferred graphene, this method is intrinsically scalable, reproducible, and compatible with the current semiconductor process, and is beneficial to the industrialization of GaN-graphene optoelectronic devices, where the integrated graphene serves as a sustainable and functional superior substitute to ITO.

Keywords: Graphene, GaN LEDs, transfer-free, lithography-free, transparent electrodes, heat spreaders

1. Introduction

As a representative of the third-generation semiconductors, gallium nitride (GaN) is a direct and wide bandgap (3.4 eV) semiconductor used extensively in a variety of optoelectronic devices that emit optically in the green, blue, and ultraviolet ranges [ref]. GaNs high breakdown voltage has made it well suited to high-power applications [ref], with typical applications including high-brightness light-emitting diodes (LEDs) [1], laser diodes [2], solar cells [3] and high-electron-mobility transistors [4]. As p-doping GaN is difficult, indium tin oxide (ITO) is often used as transparent electrode material to improve both current spreading and current injection [5-8]. Graphene is a two-dimensional material made up of sp^2 carbon atoms, which was first isolated by the Geim research team [9] in 2004 by mechanical exfoliation of bulk graphite. Single-layer graphene is only 0.335 nm thick,. Demonstrating broad and flat band optical transmission of up to 97.7% [ref], single layer graphene is highly suited for light emission applications and has an electron mobility of up to $250000 \text{ cm}^2\text{V}^{-1}\text{s}^{-1}$ at room temperature [ref]. This makes it a competitive candidate for future applications in optoelectronics, and in the near-term as a complementary, or viable

replacement to ITO. Graphene has a higher transparency in broad band, from ultraviolet to infrared and has a thermal conductivity of more than 500 times larger, with thermal conductivities of graphene of up to $5000 \text{ W}/(\text{m}\cdot\text{K})$ [ref]. Most importantly, graphene is fundamentally more sustainable than ITO, as indium is increasingly scarce and expensive. Finally, the graphene preparation process is relatively simple and cheap, and in acid or alkali environment it has higher stability. Therefore, for the application in optoelectronic devices, graphene provides much more possibilities than ITO.

Offering the most opportunities for industrial deployment, copperfoil based catalysis of graphene by chemical vapor deposition (CVD) is to-date one of the most widely reported methods for the production of highly-crystalline, large-grain, polycrystalline large-area graphene films [12-15]. However, the highly catalytically active substrates used to support graphene growth are rarely appropriate for most final applications of the material. This drives the need to transfer the graphene. A technically complex and inefficient process, graphene transfer requires skilled users who manually transfer samples. Automated transfer has recently been demonstrated [ref, ref] and though increasing throughput nonetheless continues to produce transferred graphene that is wrinkled, holey, folded, and that is often contaminated which augments, sometimes significantly [ref, ref], the electronic character of the as-synthesised graphene. In addition to this, the large work function mismatch between p-GaN ($\sim 7.5 \text{ eV}$ [ref]) and CVD graphene ($\sim 4.8 \text{ eV}$ [ref]), it is particularly difficult to establish an ohmic contact [18]. As a result, the ability to directly grow graphene, in-situ on the GaN will obviate the need for transfer, and in doing so establish a new and technologically valuable method for establishing highly electron transparent electronic contacts, that have negligible contamination. This approach lays important foundations towards to integration of graphene with CMOS technologies and has demonstrable value to a variety of other applications including XXXXXXXX. Although vital for integration, the in situ growth of graphene and GaN is very rarely reported in the literature due to what are considered incompatible growth conditions of GaN and graphene. Though graphene's unique properties technologically complement those of GaN, the high temperature ($\sim 1000^\circ\text{C}$) growth conditions required for in situ graphene growth have been seen to drive buckling and decomposition of the GaN substrate [18]. These trends are notable exacerbated under hydrogen atmospheres [ref] which are essential for amorphous carbon etching [ref], and the production of highly graphitic films during graphene synthesis. Some progress has been made in reducing the temperature for graphene synthesis [ref,ref], though often at the expense of a reduction in the graphene's crystallinity, and hence optoelectronic properties. GaN is produced at high temperatures ($\sim \text{XXXX}^\circ\text{C}$) by metalorganic chemical vapor deposition (MOCVD), but it is stable due to the $\text{Ga}(\text{CH}_3)_3$ and excess NH_3 environment which prevents decomposition,. Establishing such an environment during graphene CVD would prevent graphene formation. In order to solve this issue, in this paper, we have used several strategies to deposit transfer-free highly crystalline graphene onto GaN without compromising the GaN epitaxial wafers. To achieve this, we have successfully reduced the graphene deposition temperature to as low as 600°C whilst maintaining a D/G Raman intensity of The graphene deposition time has also been dramatically reduced, achieving full coverage of our catalytically active sites within as little as 2 minutes, based on a unique rapid-CVD system specifically designed PE-CVD for integrative growth tool to support temperature reduction during sacrificial cobalt (Co) catalysis. Collectively, this new methodology has, for the first time, allowed for the in-line, foundry compatible, direct in situ deposition of high quality graphene on GaN substrates and in doing so offers a much needed solution to an industry wide challenge.

Apart from copper, other metal such as platinum, nickel and cobalt are effective catalysts and have been shown to be able to support the growth of single- and multi-layered graphene [19-24]. These metals generally are generally more catalytically active than Cu, and are well-suited to supporting the creation of new low-temperature graphene growth protocols. However, their high carbon solubility and tendency for significant carbon precipitation has made it challenging to realise reproducible and spatially uniform deposition. The use of bi-metallic alloys has been used to inhibit carbon precipitation in this, and other overly catalytically active metals [ref], however such approaches necessarily compromise the temperature reductions attainable. The ability to grow highly crystalline graphene at technologically viable temperatures that support multi-technology integration remains elusive. In this work, pre-patterned Co is used as a sacrificial layer to locally catalyse graphene growth. Importantly, the patterned Co here was also used as a dry etching mask to produce the GaN mesas. This dual function of the Co makes the outlined methodology unique and offers the ability to pattern both the GaN mesa and the graphene electrodes within a single pattern transfer. No additional lithographic processed are required to pattern the graphene, eliminating often deteriorating process associated with the photoresist induced contamination and doping of the graphene [25]. Co was finally removed by penetration etching , as reported herein. Based on this new process flow, we have patterned high-quality graphene grown in situ on commercial GaN LED epiwafers by plasma enhanced CVD (PECVD) using sacrificial Co catalysts. The process is repeatable, controllable, scalable and fully compatible with today's semiconductor planar process, without compromising the properties of the as-synthesised graphene associated with additional transfer and patterning processes. Scanning electron microscopy (SEM), Raman spectroscopy, electroluminescence (EL) spectroscopy, and thermal distribution measurements showed that the GaN-graphene LEDs have, herein, evidence notable advantages of the graphene-free GaN LEDs over conventional manually-transferred samples. The results represent an important solution required for the integration of graphene with incumbent technologies, towards developing new hybridgraphene- GaN optoelectronics.

2. Experimental procedures

Commercial GaN LED epitaxial wafers grown on sapphire(SUPPLIER NAME? WAFER IDENTIFIER / PART NUMBER?) were used as-received. Figure 1 depicts the LED fabrication process flow . All substrates were first cleaned in acetone heated to ??Oc, and rinsed in IPA and deionized water. A 200 nm Co (99.995% purity) thin film was then deposited and patterned on the GaN (Figure 1a) as a dry etching mask by lift-off lithography and sputtering, to define an array of $260 \times 515 \mu\text{m}^2$ mesas. Samples were then placed into an inductively coupled plasma (ICP) dry etched, using SiCl_4 and Cl_2 at 8:64 to through etch the GaN and xxxx quantum wells (MQW) to a depth of 1.2 μm to reach the heavily doped n-GaN etch stop, as shown in Figure 1b. After forming the mesa array, graphene was grown on the patterned Co by cold-walled PECVD (Aixtron, Black Magic) at 600 °C at 6 mbar under a $\text{CH}_4/\text{H}_2/\text{Ar}$ (5 /20 /960 sccm) atmosphere. Figure 2a shows a schematic of the graphene growth system. Figure 2b shows an optical micrograph of the plasma during growth on a 2-inch GaN wafer.

In order to investigate the effect of growth time and plasma power on the graphene quality, 4 samples were grown for 2 min at 0, 10, 40, and 100 W AC (15kHz) plasma, and 4 additional samples grown for 20 s, 1, 2, 5 min at 40 W AC (15 kHz) plasma, respectively. Raman spectra were acquired

using a MAKE AND MODEL spectrometer operated at an excitation of ... nm, with samples measured in triplicate at xxxx points on each sample. Figures 2c and 2d show the Raman spectra for the 8 samples measured with 532 nm laser excitation.

Having obtained the patterned graphene on the Co, the Co needs to be removed so as to make the LED functional. Prior to its removal, a PMMA (poly(methyl methacrylate)) polymer layer was coated onto the sample and baked at 150°C for 15 min. In our previous work [ref], we found that the etching solution CuSO_4 : HCl : H_2O 10 g: 50 mL: 50 mL effectively removes the Co without removing the graphene [26]. The PMMA thin film is contiguous. It is attached to both the graphene and GaN well bottoms. Thus, following complete Co dissolution, the PMMA mechanically binds the graphene to the wafer ensuring that it naturally lands on the surface of the p-GaN rather than floating away in the etching solution (Figure 1f). The PMMA was then removed in xxxxxxxxxxxxxxxxxxxx, and patterned graphene directly on the p-GaN is attained, and the physical contact of graphene to any photoresist was avoided. Ti/Au (15 nm/300 nm) p and n metal electrodes were then fabricated by lift-off lithography and sputtering exterior to the graphene coated areas of the sample. In order to make a better contact among the metal electrodes, graphene, and p- or n-GaN, we annealed the final samples at 450 °C for 5 min under vacuum. Annealing LEDs were then bonded to a header package (package type???), encapsulated (PACKAGE NAME??? TO?????), as shown in Figure 1h.

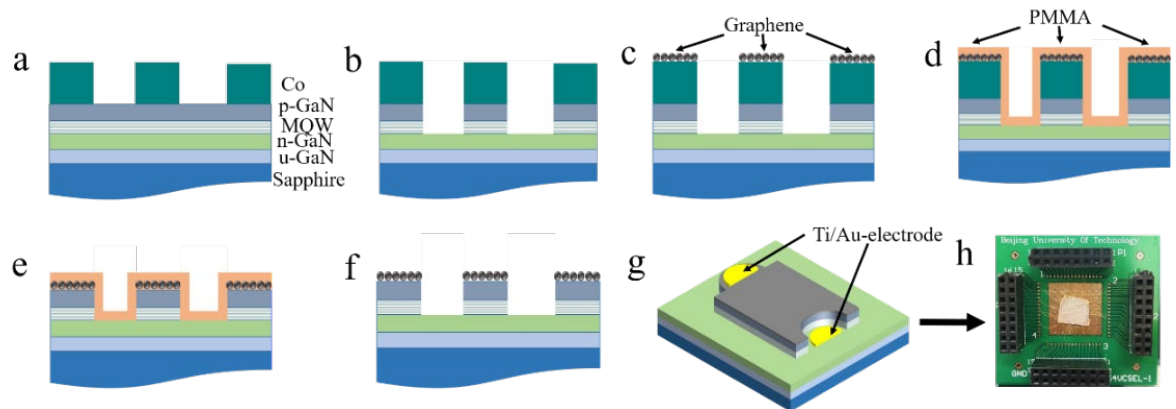


Figure 1. GaN LED transfer-less graphene integration process flow. (a) Patterned 200 nm Co by lift-off lithography and sputtering. (b) Dry etched GaN wafer to reach the heavily doped n-GaN layer. (c) Patterned graphene grown in situ on the Co catalyst. (d, e, f) Schematic illustration of the Co removal process. (g) Fabrication of Ti/Au (15 nm/300 nm) p and n metal electrodes by lift-off lithography and sputtering. (h) Wire bonding and packaging diagram of the LEDs. MQW represents multiple quantum well.

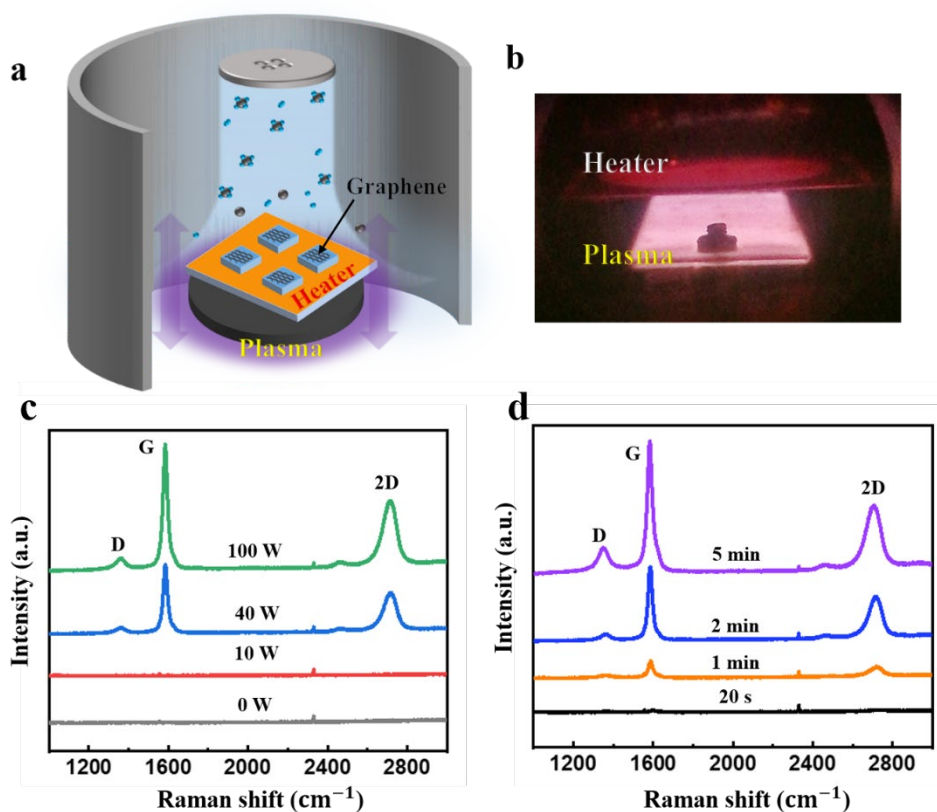


Figure 2. (a) The graphene PECVD growth schematic. The gas ratio was methane : hydrogen : argon = 5:20:960. The growth temperature and chamber pressure are fixed at 600 °C and 6 mbar, respectively. (b) Photograph taken during the actual PECVD of graphene on GaN LED wafers, showing the glow map. (c) Typical Raman spectra of the graphene subject to different AC (15 kHz) plasma power for 2 minute deposition time. (d) Raman spectroscopy comparison of the graphene grown at different times with 40 W plasma.

3. Results and Discussion

As shown from Figure 2c, plasma power tended not only to allow graphene synthesis or not, but also played an important role in determining how defective the graphene synthesized was. Characteristic graphene spectral peaks did not appear until the plasma power reached 40 W, corresponding to the position of G and 2D peaks at 1585 cm⁻¹ and 2719 cm⁻¹ respectively. The G and 2D peaks of the graphene grown at 100 W plasma are located at 1584 cm⁻¹ and 2715 cm⁻¹, respectively, which are almost identical to the former case. The intensities of these peaks, however, are known to reflect the graphene quality as well as the number of layers [ref, ref]. Increasing plasma power increased the I(G)/I(2D) ratio from 1.67 (40 W) to 1.80 (100 W), confirms that the graphene thin films grown at 100 W might be slightly nominally thicker. The I(D)/I(G) ratio in both cases are approximately equal at 0.10. The I(D)/I(G) ratio is a known signature of the defect level [27]. A I(D)/I(G) ratio of 0.10 is equivalent with standard Cu-catalyzed graphene grown at 1000 °C [28]. Thus, our results indicate that under our condition, in order to produce high quality graphene thin films at 600 °C, the plasma power needs to be reasonably large. A further increase in the plasma power leads to slightly thicker graphene with similar crystalline quality.

Figure 2d shows the graphene Raman spectra at different growth times with a 40 W AC plasma. No spectra could be acquired until the growth time reached 1 min, upon which time distinct G (1586

cm^{-1}) and 2D (2717 cm^{-1}) peaks appeared and suggesting the formation of a graphitic thin film. For the growth time of 2 min, the G peak and 2D peaks can be clearly observed at 1583 cm^{-1} and 2720 cm^{-1} , while for 5 min they appear at 1583 cm^{-1} and 2707 cm^{-1} . A comparison of the intensity ratio $I(\text{G})/I(2\text{D})$, $1.94 (5 \text{ min}) > 1.67 (2 \text{ min}) > 1.46 (1 \text{ min})$, indicates that the graphene thickness increases over time. For longer deposition times the effect D peak intensity tends to increase, possibly suggesting an increase in defects as a function of time possibly due to an increasing number of grain boundaries.

The graphene growth gas composition, temperature, and pressure have been systematically studied experimentally, and will be reported elsewhere. The optimal graphene growth conditions were found to be $600 \text{ }^\circ\text{C}$, 6 mbar, with 100 W AC (15 kHz) plasma for 2 min, in a gas mixture of 5 sccm CH_4 , 20 sccm H_2 and 960 sccm Ar. At these conditions a balance between the best possible graphene quality and maintain the intactness of the GaN epitaxial layers and device structure were reached. Figures 3a and 3b show an optical microscope image and SEM image of samples synthesized under the identified optimal conditions, respectively. The surface of the GaN epiwafer is seen to be intact. The graphene is continuous and covers the underlying p-GaN. In Figure 3a, the lower left corner of the graphene is intentionally delaminated in order to make the p-GaN beneath visible. Figure 3c represents the light transmission of the sample, where an average transparency of about 90% in the 400-1000 nm range is observed. In that measurement, the graphene-free sample was recorded first, and subtracted from the GaN-graphene sample. Hence, what is illustrated in Figure 3c is the value of bare graphene transparent conducting layer.

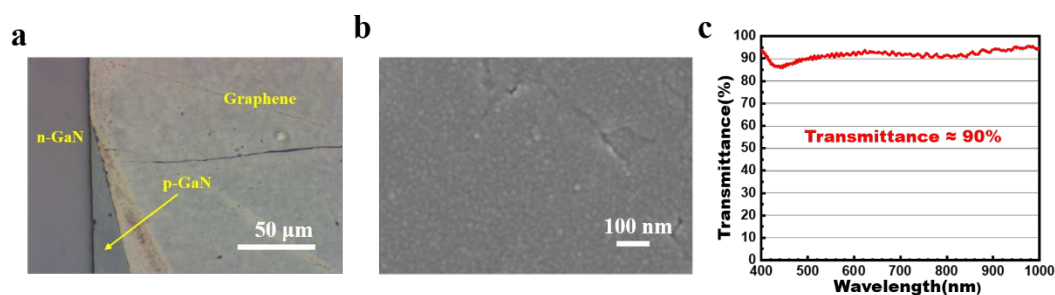


Figure 3. (a) Optical image of the as-grown graphene grown on the p-GaN. (b) SEM image of the graphene on the p-GaN. (c) Transparencies of graphene transparent electrode situated on top of the GaN LEDs (substrate transmittance already subtracted) in the 400-1000 nm range.

For graphene CVD, higher temperature give rise to higher crystallinity, increased growth uniformity, and increased grain size [ref, ref]. Nevertheless, GaN epitaxial layers are vulnerable to high temperature due to decomposition and indium segregation [ref, ref]. Throughout our experiments, we have not noticed any deterioration of the GaN epiwafers, indicating that we have obtained a good balance between the quality graphene growth and the GaN intactness. To achieve this the graphene growth temperature was reduced to $600 \text{ }^\circ\text{C}$ which built on our earlier work on the growth of graphene-like thin films on GaN [15]. During this earlier work, high growth temperatures of up to $950 \text{ }^\circ\text{C}$ were used, which was optically noted to damage the GaN. To obviate this issue in part, a NH_3 protection atmosphere was employed deriving a NH_3 -rich graphene growth environment. This compromised the quality of the synthesized carbonaceous material, resulting in a nano-graphitic matrix. WThis stimulated exploration of alternative methods to realise in-situ

growth of graphene on GaN. In the present work we opted to engineer the growth temperature within this indicative limit. Another important aspect of the outlined successful growth protocol is the short deposition time of just 2 minutes. Our SEM data suggests a lateral growth rate of+/-nm/s, which is one of the fastest growth rates reported to date, and is orders of magnitude faster than conventional Cu mediated graphene CVD. The graphene growth was extremely fast as compared to standard graphene growth processes. The entire graphene growth process, including pump down, heating, cooling and venting, takes less than 10 min. Third, we used PEVCD to provide extra energy to the precursor molecules so that they could efficiently crack even at reduced temperatures, which helped to boost the graphene quality. Co has been shown to be an effective catalyst for the production of graphitic carbon [REF from CNTs, Ref for graphene]. Our work leverages this support growth temperature reduction. Although not commonly used, Co catalyst are effective high-quality graphene growth catalysts [30]. No Co / p-GaN alloys were found under our conditions. However, even if there existed small amount of Co-GaN alloy that could not be totally removed, it would not be harmful to the operation of the device as it would support the creation of good Ohmic contacts [31]. Co is a known p-type dopant to GaN which confirms GaN's tolerance, at least to some extent, of Co alloying. [32] and it is this that, in part, was a founding rationale for the use of Co as the graphene catalyst here.

THERE SHOULD BE A paragraph here reporting data on the GaN METROLOGY BEFORE AND after Gr growth

For comparison study, GaN LED devices without any graphene was also fabricated with an otherwise similar process. The current-voltage (I - V) curve comparison between GaN-graphene and GaN without graphene LEDs is shown in Figure 4. The turn-on voltages of the GaN-graphene LED and the graphene-free GaN LED are about 3.8 V and 8.2 V, respectively, while the working voltage at 20 mA are about 4.1 V and 7.8 V, respectively. Use of graphene tends to reduce the required device voltages. In addition, the GaN-graphene LED reached 100 mA at 6.2 V, however the same current level can in the graphene-free GaN LED is only reached at 8.8 V. The inset shows the corresponding optical images of the light emission at 20 mA, suggesting that the GaN-graphene LED illuminates more uniformly, and the light emitting area covers the entire p-GaN mesa, while the LED without graphene has only a single light emission point located close to the p-electrode, a common effect in higher-driving voltage devices. The as-prepared graphene serves to enhance the functionality of the GaN LED by operating as an effective transparent conductive layer. The graphene transparent electrode shows an excellent current spreading effect, i.e. greatly improving the conductivity of the GaN LEDs.

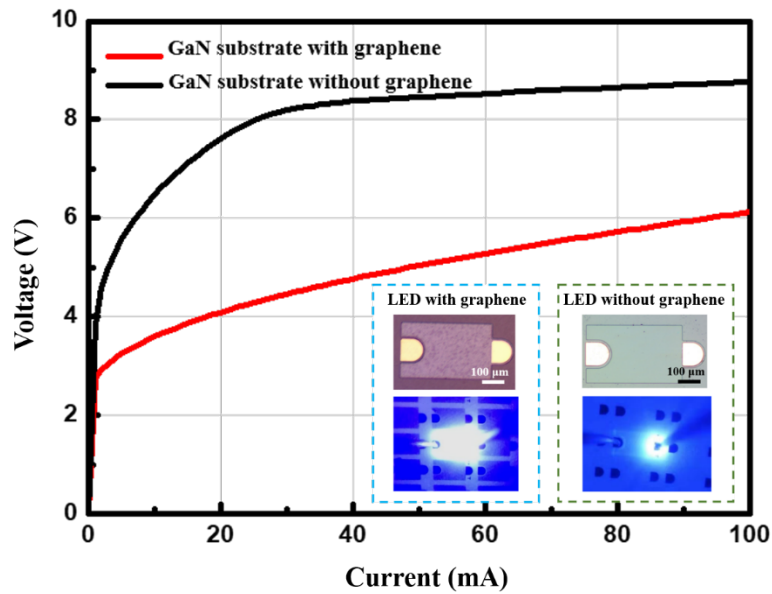


Figure 4. A current–voltage curve comparison of the LED devices with and without graphene transparency conductive layer (after annealing). The inset shows the corresponding optical images of light emission at 20 mA.

Further quantitative data about the optoelectronic properties of the graphene on GaN LEDs was explored via electroluminescence (EL) spectroscopy (Integrating sphere, EVERFINE) on the with and without graphene samples operated with injection currents of 20 mA and 100 mA, respectively, to ensure optically commensurate emission intensity in both cases. Figure 5a and 5b shows the EL spectra from the GaN-graphene LED. Figure 5c and 5d show the EL spectra from the graphene-free GaN LED, both measured in the 380-780 nm range. The GaN-graphene LED, at the same injection current, is superior to the graphene-free GaN LEDs in the luminous flux and radiation flux. More specifically, the luminous flux values of the GaN-graphene LED are nearly twice as high as the graphene-free GaN LED at 20 mA and 100 mA, which indicates the outstanding electrical to optical energy conversion efficiency in the GaN-graphene LED. In all samples there is a notable blue shift of the order of ??? nm in the peak emission wavelength. This is a known effect that is due to the high built-in electric field (of the order of few MV/cm) along the (0001) direction of InGaN/GaN quantum well [33], which induces the quantum confined Stark effect (QCSE) and leads to a red shift in the wavelength. When the injected current becomes large, due to the relatively long lifetime of the carriers (in the order of ns), they will accumulate in the quantum well, leading to a built-up of an electron-hole plasma that screens the built-in field [34]. That results in a blue shift partly compensating the red shift induced by QCSE, and the large injection current induced blue shift is hence explained. The blue shift from Figure 5a to 5c and from Figure 5b to 5d can be interpreted similarly by the pronounced carrier injection effect. Due to its low sheet resistance, the graphene-free sample cannot current spread effectively, at the same current level, the current crowding leads to a very large local current density in the LED. As shown in Figure 5, the pristine GaN LED has a smaller half-wave width. Nevertheless, we note that it is not because the graphene-free devices perform better, but rather because only one point is emitting light on the p-GaN mesa there.

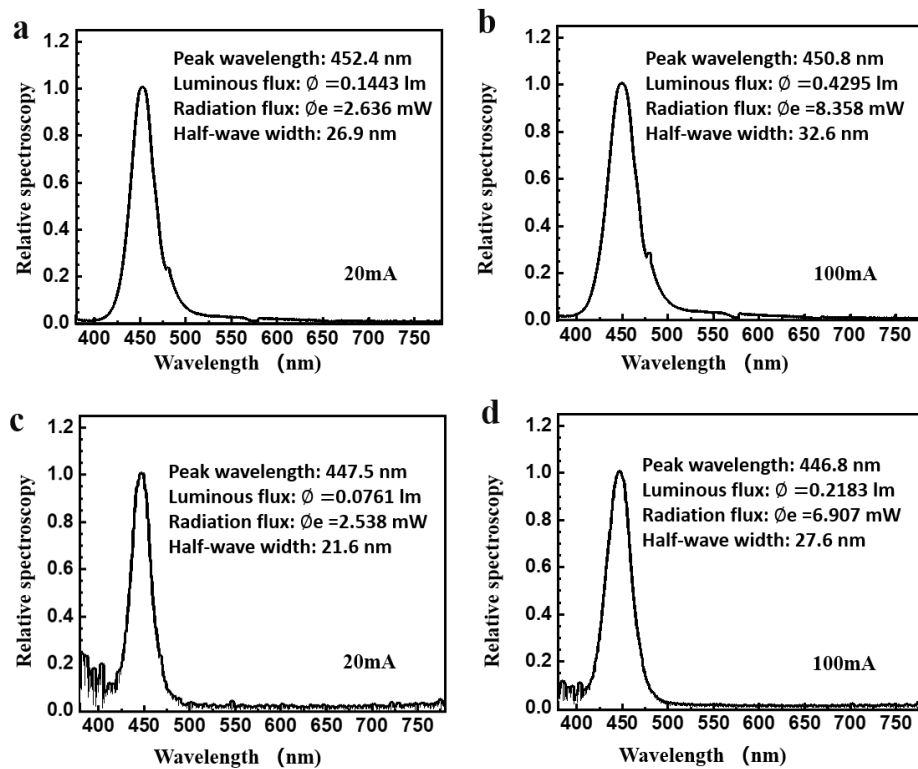


Figure 5. Electroluminescence spectra of GaN LEDs at 20 mA and 100 mA injection current in the 380-780 nm range. (a, b) GaN-graphene LED. (c, d) GaN LED without graphene.

EXPLAIN WHY HIGHER OPERATING TEMPERATURES IN LEDs IS A BAD THING
 FIRST – do higher operating temperatures reduce the lifetime of LEDs (if so, why/how)? Does it make them less efficient? . Graphene is believed to have the highest thermal conductivity of any known, and presently synthesisable materials [ref, ref, ref]. It has shown demonstrable potential as an effective heat sink in various thermal applications [ref, ref] . Unlike ITO, graphene has a high potential as the heat spreader in LEDs. Compare the actual value of THERMAL CONDUCTIVITY OF Gr [ref] and ITO [REF]. Graphene has the potential to positively augment the thermal management of GaN LEDs, which is explored here. Figure 6 shows thermal maps (SC7300M F/2 (MCT) thermal imaging camera FLIR Systems) of the coated and uncoated LEDs operating at 0 mA (no optical emission, room temperature), 20 mA, and 100 mA in constant current mode. At 20 mA , the temperature increase of the GaN-graphene LED was 00.83 °C compared to room temperature (RT). The pristine GaN LED increased by 1.14 °C. Integrating graphene reduced the temperature increase by a significant 22.8%. When the temperature was raised to 100 mA, the GaN-graphene LED temperature increased by 11.13 °C, while the graphene-free GaN LED increased by 13.98 °C. Clearly, there is a thermal spreading effect from the graphene. We conclude that the as-grown graphene has played a significantly positive role in the cooling of GaN LEDs, both at small or high current, but with a more pronounced effect towards higher injection current in particular. The results indicate that our directly grown graphene technology may be especially useful for high power density GaN based LEDs.

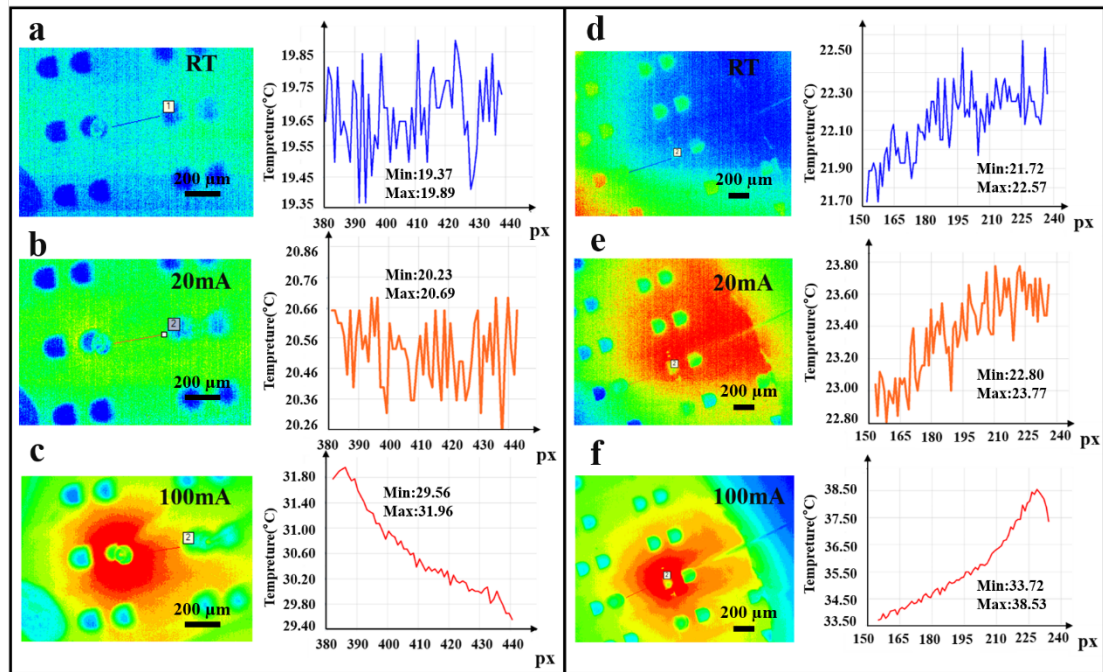


Figure 6. Thermal maps of the GaN LEDs at room temperature (RT, 0 mA), 20 mA and 100 mA. (a, b, c) GaN-graphene LED. (d, e, f) GaN LED without graphene..

4. Conclusion

Here we have demonstrated, for the first time, a practical and deployable method for the production of transfer-free patterned graphene directly grown on GaN LED epiwafers. The developed process has been seen to be GaN compatible through the use of low graphene synthesis temperatures of only $600\text{ }^{\circ}\text{C}$ and the use of dual-functionality Co which catalyses graphene growth but also functions as an effective MQW etching hard mask, which greatly simplifies the complicated problem of graphene transfer process in traditional fabrication process., improving device yield. The graphene growth temperature was reduced by virtue of the plasma enhancement technique, and our vertical cold wall CVD system offered the possibility of growing graphene in merely 2 min. From the study on the effects of different plasma powers and growth time, we have confirmed that 2 min and 40 W AC (15 kHz) plasma were the best growth conditions for the PECVD of graphene. Consequently, high-quality graphene was obtained on the GaN LED epiwafers with average optical transmission of 90%, and the entire graphene growth process (even including heating and cooling) took less than 10 min. Comprehensive electrical, optical and thermal analysis of the GaN-graphene LEDs produced by this method have been conducted. Integrated GaN-graphene LEDs demonstrated improved current spreading, current injection and heat spreading functions. Unlike other work on graphene application in GaN optoelectronic devices, this facile method is fundamentally scalable, reproducible, controllable, and compatible with current GaN processing, which is suitable for mass device production towards real applications whilst contributing to the deployment of graphene as a sustainable ITO alternative.

Acknowledgment

This work was supported by the National Natural Science Foundation of China (11674016), National

Key R&D Program of China (2018YFA0209004 and 2017YFB0403102), and Beijing Municipal Commission of Education (KM201810005029).

References

- [1] Chichibu, S.F.; Uedono, A.; Onuma, T.; Haskell, B.A.; Chakraborty, A.; Koyama, T.; Fini, P. T.; Keller, S.; DenBaars, S.P.; Speck, J.S.; et al. Origin of defect-insensitive emission probability in In-containing (Al, In, GaN) alloy semiconductors. *Nature Mater.* **2006.** 5, 10, 810–816.
- [2] Nakamura, S. The roles of structural imperfections in InGaN-based blue light-emitting diodes and laser diodes. *Science.* **1998.** 281, 5379, 956–961.
- [3] Lang, F.; Gluba, M.A.; Albrecht, S.; Rappich, J.; Korte, L.; Rech, B.; Nickel, N.H. Perovskite Solar Cells with Large-Area CVD-Graphene for Tandem Solar Cells. *J. Phys. Chem. Lett.* **2015.** 6, 14, 2745-2750.
- [4] Mishra U.K.; Parikh, P.; Wu, Y. AlGaIn/GaN HEMTs—an overview of device operation and applications. *Proc. IEEE.* **2002.** 90, 6, 1022-1031.
- [5] Wu, K.; Wei, T.; Lan, D.; Zheng, H.; Wang, J.; Luo, Y.; Li, J. Large-scale SiO₂ photonic crystal for high efficiency GaN LEDs by nanospherical-lens lithography. *Chin. Phys. B.* **2014.** 23, 028504.
- [6] Amano, H.; Kito, M.; Hiramatsu K.; Akasaki, I. P-type conduction in Mg-doped GaN treated with low-energy electron-beam irradiation (LEEBI). *Jpn. J. Appl. Phys.* **1989.** 28, 2112–2114.
- [7] Nakamura, S.; Mukai, T.; Senoh, M.; Lwasa, N. Thermal annealing effects on p-type Mg-doped GaN films. *Jpn. J. Appl. Phys.* **1992.** 31,139–142.
- [8] Neugebauer, J.; Vandewalle, C. G. Role of hydrogen in doping of GaN. *Appl. Phys. Lett.* **1996.** 68, 1829–1831.
- [9] Novoselov, K.; Geim, A.; Morozov, S.; Jiang, D.; Zhang, Y.; Dubonos, S.; Grigorieva, I.; Firsov, A. Electric field effect in atomically thin carbon films. *Science.* **2004.** 306, 666–669.
- [10] Lee, C.; Wei, X.; Kysar, J. W.; Hone, J. Measurement of the elastic properties and intrinsic strength of monolayer graphene. *Science.* **2008.** 321, 5887, 385-388.
- [11] Bonaccorso, F.; Sun, Z.; Hasan, T.; Ferrari, A.C. Graphene photonics and optoelectronics. *Nat Photon.* **2010.** 4, 611–622.
- [12] Zhan, Z.; Sun, J.; Liu, L.; Wang, E.; Wang, E.; Cao, Y.; Lindvall, N.; Skoblin, G.; Yurgens, A. Pore-Free Bubbling Delamination of Chemical Vapor Deposited Graphene from Copper Foils. *J. Mater. Chem. C.* **2015.** 3, 8634–8641.
- [13] Sun, J.; Lindvall, N.; Cole, M.T.; Angel, K.T.T.; Wang, T.; Teo, K.B.K.; Chua, D.H.C.; Liu, J.; Yurgens, A. Low partial pressure chemical vapor deposition of graphene on copper. *IEEE Trans. Nanotechnol.* **2012.** 11, 255–260.
- [14] Kim, B.J.; Lee, C.; Jung Y.; Baik, K.H.; Mastro, M.A.; Hite, J.K.; Eddy Jr, C.R.; Kim, J. Large-area transparent conductive few-layer graphene electrode in GaN-based ultra-violet light-emitting diodes. *Appl. Phys. Lett.* **2011.** 99, 143101.
- [15] Sun, J.; Cole, M.T.; Ahmad, S.A.; Backe, O.; Ive, T.; Loffler, M.; Lindvall, N.; Olsson, E.; Teo, K.B.K.; Liu, J.; et al. Direct chemical vapor deposition of large-area carbon thin films on gallium nitride for transparent electrodes: A first attempt. *IEEE Trans Semicond. Manuf.* **2012.** 25, 494–501.
- [16] Cabrero-Vilatelá, A.; Weatherup R.S.; Braeuninger-Weimer, P.; Caneva, S.; Hofmann, S.

Towards a General Growth Model for Graphene CVD on Transition Metal Catalysts. *Nanoscale*. **2016**. 8, 4, 2149-2158.

- [17] Li, X.; Cai, W.; Colombo, L.; Ruoff, R.S. Evolution of graphene growth on Ni and Cu by carbon isotope labeling. *Nano Lett.* **2009**. 9, 4268–4272.
- [18] Zhao, Y.; Wang, G.; Yang, H.; An, T.; Chen, M.; Yu, F.; Tao, L.; Yang, J.; Wei, T.; Duan, R.; et al. Direct growth of graphene on gallium nitride by using chemical vapor deposition without extra catalyst. *Chinese Physics B*. **2014**. 23, 9, 096802.
- [19] Weatherup, R. S.; Dlubak, B.; Hofmann, S. *ACS Nano*. **2012**. 6, 9996–10003.
- [20] Gao, L.; Ren, W.; Xu, H.; Jin, L.; Wang, Z.; Ma, T.; Zhang, Z.; Fu, Q.; Peng, L.; et al. Repeated growth and bubbling transfer of graphene with millimetre-size single-crystal grains using platinum. *Nat. Commun.* **2012**. 3, 699.
- [21] Xiong F.; Guo W.; Feng S.; Li, X.; Du Z.; Wang, L.; Deng, J.; Sun, J. Transfer-Free Graphene-Like Thin Films on GaN LED Epiwafers Grown by PECVD Using an Ultrathin Pt Catalyst for Transparent Electrode. *Materials*. **2019**. 12, 21.
- [22] Sun, J.; Nam, Y.; Lindvall, N.; Cole, M.T.; Teo, K.B.K.; Park, Y.W.; Yurgens, A. Growth mechanism of graphene on platinum: Surface catalysis and carbon segregation. *Appl. Phys. Lett.* **2014**. 104, 152107.
- [23] Weatherup, R.S.; Bayer, B.C.; Blume, R.; Ducati, C.; Baehtz, C.; Schlögl, R.; Hofmann, S. In Situ Characterization of Alloy Catalysts for Low-Temperature Graphene Growth. *Nano Letters*. **2011**. 11, 10, 4154-4160.
- [24] Weatherup, R.S.; Bayer, B.C.; Blume, R.; Baehtz, C.; Kidambi, P.R.; Fouquet, M.; Wirth, C. T.; Schlögl, R.; Hofmann, S. On the Mechanisms of Ni-Catalysed Graphene Chemical Vapour Deposition. *ChemPhysChem*. **2012**. 13, 2544–2549.
- [25] Sul, O.; Kim, K.; Choi, E.; Kil, J.; Park, W.; Lee, S.B. Reduction of hole doping of chemical vapor deposition grown graphene by photoresist selection and thermal treatment. *Nanotechnology*. **2016**. 27(50), 505205.
- [26] Dong, Y.; Guo, S.; Mao, H.; Xu, C.; Xie, Y.; Deng, J.; Wang, L.; Du, Z.; Xiong, F.; Sun, J. In Situ Growth of CVD Graphene Directly on Dielectric Surface toward Application. *ACS Appl. Electron. Mater.* **2020**. 2, 238–246.
- [27] Lucchese, M.M.; Stavale, F.; Ferreira, E.H.M.; Vilani, C.; Moutinho, M.V.O.; Capaz, R.B. Quantifying ion-induced defects and raman relaxation length in graphene. *Carbon*. **2010**. 48(5), 1592-1597.
- [28] Rosa, C.J.; Sun, J.; Lindvall, N.; Cole, M.T.; Nam, Y.; Loeffler, M.; Olsson, E.; Teo, K.B.K.; Yurgens, A. Frame assisted H₂O electrolysis induced H₂ bubbling transfer of large area graphene grown by chemical vapor deposition on Cu. *Appl. Phys. Lett.* **2013**. 102, 22101.
- [29] Xu, K.; Xu, C.; Deng, J.; Zhu, Y.; Guo W.; Mao, M.; Zheng, L.; Sun, J. Graphene transparent electrodes grown by rapid chemical vapor deposition with ultrathin indium tin oxide contact layers for GaN light emitting diodes. *Appl. Phys. Lett.* **2013**. 102(16), 666.
- [30] Mehedi, H.-A.; Baudrillart, B.; Alloeyau, D.; Mouhoub, O.; Ricolleau, C.; Pham, V. D.; Chacon, C.; Gicquel, A.; Lagoute, J.; Farhat, S. Synthesis of graphene by cobalt-catalyzed decomposition of methane in plasma-enhanced CVD: Optimization of experimental parameters with Taguchi method. *J. Appl. Phys.* **2016**. 120, 065304.
- [31] Wenzel, Roland.; Fischer, Gerhard G.; Schmid Fetzer, Rainer. Ohmic contacts on p-GaN (Part I):: investigation of different contact metals and their thermal treatment. *Mater Sci Semicond*

Process. **2001.** 4(4):357-365.

- [32] Sawahata, J.; Bang, H.; Takiguchi, M.; Seo, J.; Yanagihara, H.; Kita, E.; Akimoto, K. Structural and magnetic properties of Co doped GaN. *Phys. stat. sol. (c)*. **2005.** 2: 2458-2462.
- [33] Dutt, M. B.; Mittal, V. Investigation of electrical transport properties of as-implanted silicon for making micromachined uncooled bolometric arrays. *J. Appl. Phys.* **2005.** 97, 083704.
- [34] Traetta, G.; Carlo, A. D.; Reale, A.; Lugli, P.; Lomascolo, M.; Passaseo, A.; Cingolani, R.; Bonfiglio, A.; Berti, M.; Napolitani, E.; et al. Charge storage and screening of the internal field in GaN/AlGaIn quantum wells. *J. Cryst. Growth.* **2001.** 230, 492-496.